AN ENERGY AND EXERGY STUDY OF A SOLAR THERMAL AIR COLLECTOR

by

Ehsan MOHSENI-LANGURI, Hessam TAHERIAN, Reza MASOODI, and John R. REISEL

Original scientific paper
UDC: 697.329:620.91
BIBLID: 0354-9836, *13* (2009), 1, 205-216
DOI: 10.2298/TSCI0901205M

A solar flat plate air collector was manufactured in the north of Iran, and connected to a room as the model to study the possibility of using such solar heating systems in the northern parts of Iran. This collector was tested as a solar air heater to see how good it could be for warming up the test room during the winter. The experimental data obtained through accurate measurements were analyzed using second law approach to find the optimum mass flow rate, which leads to the maximum exergy efficiency. It was found that for the test setup at the test location, a mass flow rate of 0.0011 kg/s is the optimum mass flow rate for tested conditions which leads to the highest second law efficiency.

Key words: *exergy, energy, solar collector, solar air heater, second law analysis, second law efficiency*

Introduction

The amount of solar energy striking the earth's surface depends on the season, local weather conditions, location, and orientation of the surface but it averages about 1000 W/m^2 if the absorbing surface is perpendicular to the sun's rays and the sky is clear. There are several ways of absorbing and using this free, clean, renewable, and very long lasting source of energy. Solar collectors are special devices that can absorb and transfer energy of the sun to a usable or storable form. Solar thermal collectors, which are a group of solar collectors, can be made in different shapes based on their application. Some types of thermal solar collectors, such as parabolic trough, are generally used in solar power plants where solar heat energy is used to generate electricity.

Flat plate collectors are the most common types of solar collectors and are usually used as solar hot water panels to generate hot water or as solar air heater for pre-heating the air in domestic or industrial heating, ventilation, and air conditioning (HVAC) systems. A weatherproof insulated box containing a black metal absorber sheet with built-in pipes is placed in the path of sunlight. Solar energy heats up water in the pipes causing it to circulate through the system by natural convection. The water is usually passed to a storage tank located above the collector. This passive solar water heating system is generally used in hotels and homes such as those found in southern Europe.

There are many flat-plate collector designs but generally all consist of four major parts; (1) a flat-plate absorber, which absorbs the solar energy, (2) a transparent cover(s) that allows solar energy to pass through and reduces heat loss from the absorber, (3) a heat-transport fluid (air or water) flowing through the collector (water flows through tubes) to remove heat from the absorber, and (4) a heat insulating backing.

Literature survey

The exergy of a system is the maximum useful work possible during a process that brings the system into equilibrium with a heat reservoir [1]. Exergy can be destroyed by irreversibility of a process. An exergy analysis (2^{nd} law analysis) is a very powerful way of optimizing complex thermodynamic systems. The term exergy was proposed by Rant [2] in 1956, but the concept was developed by Gibbs [3] in 1873. Nowadays, details of this concept can be found in thermodynamics texts, (*e. g.* [4-7]). Several researchers have used this powerful method to optimize different thermodynamical parameters of power plant components. As a recent application of second law analysis, Saravanan *et. al.* [8] used energy and exergy analysis to study the performance of a cooling tower.

The governing equations of exergy balance as applied to solar collectors has been published by Bejan *et al.* [9] and Bejan [10]. Recently Londono-Hurtado *et al.* [11] developed a model to study the behavior of volumetric absorption solar collectors (VASC) and the influence of the design parameters on the performance of the collectors. Their approach is based on the use of several dimensionless numbers, each of them having a clear physical significance, which play a key role in the analysis of the collector. The model is then used to conduct a thermodynamic optimization of VASC, which gives the optimal design parameters that maximize the exergy output of the heat extracted from the collector. Another notable study is the work of Luminosu *et al*. [12] where they experimentally studied an air solar installation. They processed their experimental results through thermodynamic analysis, using energy and exergy methods to find the best flow rate of passing air.

Altfeld *et al*. [13, 14] considered different solar air heater configurations including finned surface. They state that the heat transfer characteristics of the absorber are less important if highly insulated solar air heaters are considered. Torres-Reyes *et al*. [15] performed thermodynamic optimization based on first and second law to determine the optimal performance parameters and to design a solar thermal energy conversion system. They produced graphs of exergy flow rate as a function of mass flow rate for different collector configurations.

Kurtbas *et al.* [16] used five different absorber plates for solar air heater including a corrugated one. They concluded that there was a reverse relationship between dimensionless exergy loss and heat transfer, as well as pressure loss. The more important parameters in order to decrease the exergy loss are the collector efficiency, temperature difference of the air, and pressure loss. Ajam *et al*. [17] derived the equations to study the exergetic efficiency of solar air heaters and used MATLAB to optimize the system. Ucar *et al.* [18] made changes to a conventional solar air heater such as dividing its absorber plate to six parts and giving angles to them. They did an energy and exergy analysis and found that some simple modifications can increase the efficiency by up to 30%.

Esen [19] reported an experimental study to evaluate the energetic and exergetic efficiencies of four types of double-flow solar air collectors under a wide range of operating conditions. He showed that the use of obstacles in the air duct of the double-flow collector is an efficient method of adapting air exchanger according to user needs. Gupta *et al.* [20] reported exergetic performance evaluation and parametric studies of solar air heater. They stated that based on the output energy evaluation, the solar air heater should have high aspect ratio, low duct depth, and low inlet temperature of air. They have observed and proved that if the inlet temperature of air is low, then maximum exergy output is achieved at low value of mass flow rate.

Fujiwara [21] analyzed the optimum control and performance evaluation of solar collectors from exergy standpoint. He demonstrated that the maximum capability of collectors is determined and expressed by a relationship among the collector parameters and the environment in which they operate. Xiaowu *et al.* [22] conducted an exergy analysis on a domestic-scale solar water heater to optimize its thermodynamical parameters. They tried to find the major sources of irreversibilities and their relative importance for a special kind of solar water heater.

As fossil fuel price is quite high and it is expected to stay up for many years, the idea of using solar thermal collectors for warming up of houses in the northern part of Iran was considered by Mohseni-Languri [23]. In this research, a flat plate solar air heater manufactured and connected to a test room to study the practical utility and efficiency of this method for the suggested area of installation. Some of the objectives of this study are:

- determination of basic engineering characteristics of a simple and economic flat plate solar collectors for domestic users,
- feasibility study of air solar installation in the northern parts of the country,
- study the energy saving for a test room to estimate the possible energy saving for the proposed area of installation, and
- optimization of air flow rate for solar air collector using a test room.

Some of the results obtained in this study is presented here, which are focused on the second law optimization of mass flow rate of working fluid. We have measured/calculated the average solar irreversibility, average radiation intensity, average useful energy, average air temperature variation, energy efficiency, and exergy efficiency during the day for winter months. The method used by Luminosu *et al*. [12] and Esen [19] was employed to analysis the sample solar installation data. All sources of irreversibility were considered to minimize the irreversibility by optimizing the air flow rate.

Experimental study

Location of the study

The experimental study was done [23] in the north of Iran. The latitude and longitude of the location are 36°32’39"N and 52°40’44"E. The ambient temperature fluctuates in the range of 0 to 29 ºC during the year in Babol. Due to rainy or cloudy weather, we had to cross out some days, in which solar energy tests were not possible.

Table1. Technical characteristics of the collector [23]

Part name	Dimension [cm]	Material	Remark
Absorber	180 100 0.4	Carbon steel	Painted black
Insulator	4	Glass wool	Thickness
Cover	0.3	Flat glass	Thickness
Ducts	10 5	Aluminum	Inlet and exit channels

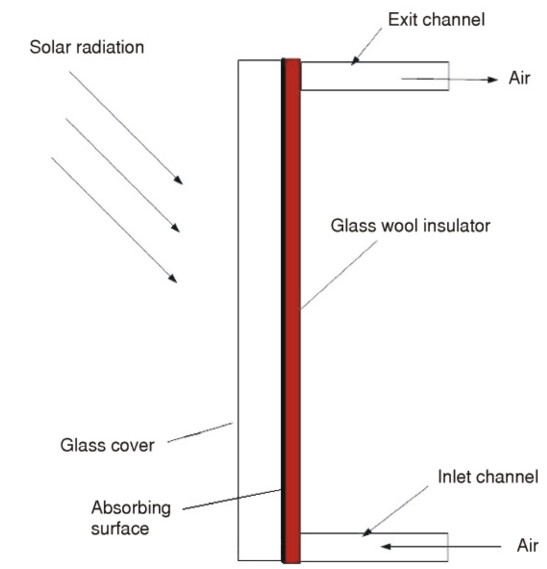

Figure 1. A schematic of the designed collector [23]

Characteristics of the testing collector

A flat solar air collector was designed to use in this study. Figure 1 shows a schematic of the design. The characteristics of the collector are summarized in tab. 1. The collector was verticaly installed at a distance of 2.5 m from the ground to prevent shading by neighborhood buildings. The inlet and exit channels were connected to the testing room through two aluminum tubes highly insulated using glass wool of 2 cm thickness. Figure 2 shows the schematic of final test setup. The test system was connected to a room of 4 m 3 m 3 m. A small fan of 40 W was used to circulate the air through the collector and room.

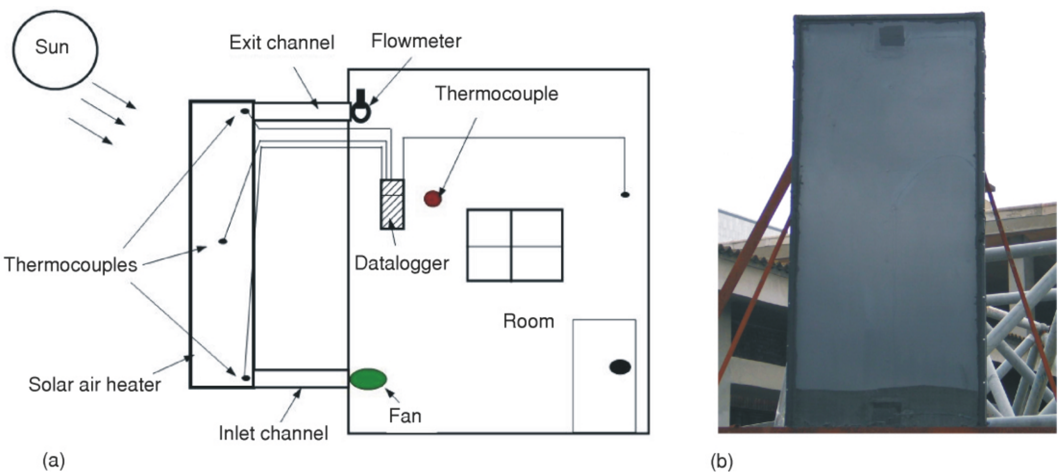

Figure 2. A schematic of test setup and photo of the collector [23]
(a) a schematic of final test setup, (b) assembled collector in its final place

Measuring devices

To measure the mass flow rate of the air, an anemometer was used to measure the speed of the air flow. As the temperature was also measured in the ducts, we were able to estimate the flow rate of the air through the channels. There were five thermocouples located in five critical positions; two thermocouples located in the inlet and outlet ducts, one attached to the absorbing surface, the other one was placed in the room, and the last one was placed outside of the room for sensing the ambient temperature (see fig. 2a). The measured temperature inside and outside the room were bulk temperature while the other temperatures were local. The accuracy of temperature measurements were ±1 °C. The solar radiation intensity has also been measured using a local weather station. All the measurement devices were connected to a data logger system, which recorded the data every 15 minutes during the test days.

All the measuring devices were calibrated before the experimental study. The statistical data about the weather showed that we will have clear sky in about 85% of the days in the winter. In this study, we had excluded the data for those days, in which the sky was cloudy and so absorbed solar radiation was different from the sunny days. It happened for 76 days during the winter of studying year.

Energy and exergy analysis

Energy analysis

Based on Duffie *et al.* [24], the rate of heat received by the heat carrier, which is air here, from the collector is:

$$\dot{Q}_{\mathrm{a}} = \dot{m}_{\mathrm{a}} C_{\mathrm{p}} (T_{\mathrm{out}} - T_{\mathrm{in}}) \tag{1}$$

The specific collector power can be found by dividing of this heat by the area of the collector [24]:

$$\dot{q}_{\mathrm{a}} = \frac{\dot{Q}_{\mathrm{a}}}{A_{\mathrm{c}}} = \frac{\dot{m}_{\mathrm{a}} C_{\mathrm{p}} (T_{\mathrm{out}} - T_{in})}{A_{\mathrm{c}}} \tag{2}$$

The average daily useful heat per unit area of the collector can be found adding up all radiation times as:

$$q_{\mathrm{a\,d}} = 3600 \sum_{i=1}^{8} \dot{q}_{\mathrm{a\,i}} \tag{3}$$

in which $\dot{q}_{\mathrm{a\,i}}$ is the useful heat per unit area of the collector for the hour i of the test day. As we started the tests at 8:00 a. m. and ended at 4:00 p. m. so i could be between 1 to 8. So the energy efficiency of solar energy that is converted to heat could be expressed by the ratio of absorbed energy to the total energy of the sun that was available [12]:

$$\eta_{\mathrm{en}} = \frac{\dot{q}_{\mathrm{a}}}{G_{\mathrm{c}}} \tag{4}$$

where G_{c} is the solar radiation captured by the collector.

Exergy analysis

Based on Bejan *et al.* [9] and Bejan [10], there are two sources of entropy generation in a solar air collector, which are entropy generation due to the friction of passing fluid, and entropy generated due to the thermal heat transfer or temperature change of the fluid flow. We did the exergy analysis using Esen's approach [19], considering following assumptions:
- the process is steady-state and steady flow,
- the potential and kinetic energies are negligible,
- air is an ideal gas, so its specific heat is constant, and
- the humidity of air is negligible.

The general exergy balance for a steady-state and steady flow process is:

$$\dot{I} = \dot{E}x_{\mathrm{heat}} - \dot{E}x_{\mathrm{work}} + \dot{E}x_{\mathrm{in}} - \dot{E}x_{\mathrm{out}} \tag{5}$$

Considering above assumptions, following relations are available for each component:

$$\dot{E}x_{\mathrm{heat}} \quad 1 \quad \frac{T_0}{T_\mathrm{s}} \quad \dot{Q}_\mathrm{s} \tag{6}$$

$$\dot{E}x_{\mathrm{work}} \quad 0 \tag{7}$$

$$\dot{E}x_{\mathrm{in}} \quad \dot{m}_{\mathrm{in}}[(h_{\mathrm{in}} \quad h_0) \quad T_0(s_{\mathrm{in}} \quad s_0)] \tag{8}$$

$$\dot{E}x_{\mathrm{out}} \quad \dot{m}_{\mathrm{out}}[(h_{\mathrm{out}} \quad h_0) \quad T_0(s_{\mathrm{out}} \quad s_0)] \tag{9}$$

Equation (7) comes from the fact that no work has done during the process. From mass balance we have:

$$\Sigma\dot{m}_{\mathrm{in}} \quad \Sigma\dot{m}_{\mathrm{out}} \quad \dot{m}_\mathrm{a} \tag{10}$$

Upon substitution of eqs. (6) to (10) in eq. (5), the rate of irreversibility will be:

$$\dot{I} \quad 1 \quad \frac{T_0}{T_\mathrm{s}} \quad \dot{Q}_\mathrm{s} \quad \dot{m}_\mathrm{a}[(h_{\mathrm{out}} \quad h_{\mathrm{in}}) \quad T_0(s_{\mathrm{out}} \quad s_{in})] \tag{11}$$

where $\dot{Q}_\mathrm{s}$ is the total rate of the exergy received by the collector absorber area from the solar radiation and is evaluated by relation:

$$\dot{Q}_\mathrm{s} \quad G_\mathrm{c}A_\mathrm{c}\tau\alpha \tag{12}$$

where $\tau\alpha$ is absorbance-transmittance product of the covering glass and the absorber plate. The changes in enthalpy and entropy of air in the collector can be obtained using following two expressions:

$$h_{\mathrm{out}} - h_{\mathrm{in}} = C_\mathrm{p}(T_{\mathrm{out}} - T_{\mathrm{in}}) \tag{13}$$

and

$$s_{\mathrm{out}} \quad s_{\mathrm{in}} \quad C_\mathrm{p} \ln\frac{T_{\mathrm{out}}}{T_{\mathrm{in}}} \quad \mathrm{R}\ln\frac{P_{\mathrm{out}}}{P_{\mathrm{in}}} \tag{14}$$

After substituting eqs. (12) to (14) in eq. (11), the final form of expression for irreversibility rate in the solar collector will be:

$$\dot{I} \quad 1 \quad \frac{T_0}{T_\mathrm{s}} \quad G_\mathrm{c}A_\mathrm{c}\tau\alpha \quad \dot{m}_\mathrm{a}C_\mathrm{p}(T_{\mathrm{out}} \quad T_{\mathrm{in}}) \quad \dot{m}_a T_0 C_\mathrm{p}\ln\frac{T_{\mathrm{out}}}{T_{\mathrm{in}}} \quad \dot{m}_\mathrm{a}T_0\mathrm{R}\ln\frac{P_{\mathrm{out}}}{P_{\mathrm{in}}} \tag{15}$$

where T_s is the apparent temperature of sun surface, which considered to be 6000 K. In this equation the first term comes from the entropy generated due to heat transfer; second and third terms are related to the temperature change of passing fluid; last term is related to the entropy generated due to the friction of fluid. By definition, irreversibility is the total entropy generated times the ambient temperature [6]:

$$\dot{I} \quad \dot{S}_{\mathrm{gen}}T_0 \tag{16}$$

Therefore, the total entropy generated during the process will be:

$$\dot{S}_{\mathrm{gen}} \quad \frac{1}{T_0} \quad 1 \quad \frac{T_0}{T_\mathrm{s}} \quad G_\mathrm{c}A_\mathrm{c}\tau\alpha \quad \dot{m}_a C_\mathrm{p}(T_{\mathrm{out}} \quad T_{\mathrm{in}}) \quad \dot{m}_\mathrm{a}C_\mathrm{p}\ln\frac{T_{\mathrm{out}}}{T_{\mathrm{in}}} \quad \dot{m}_\mathrm{a}\mathrm{R}\ln\frac{P_{\mathrm{out}}}{P_{\mathrm{in}}} \tag{17}$$

So the exergy efficiency, as defined through second law of thermodynamics [15], is:

$$\eta_{\mathrm{ex}} \quad 1 \quad \frac{\dot{I}}{\dot{E}x_{\mathrm{heat}}} \quad 1 \quad \frac{\dot{S}_{\mathrm{gen}} T_0}{1 \quad \dfrac{T_0}{T_{\mathrm{s}}} \quad \dot{Q}_{\mathrm{s}}} \tag{18}$$

Error analysis

There are two types of errors; one group come from direct measurement, which are ΔG_{c}, T, P, and $\Delta\dot{m}$; the second group of errors come from indirect measurement, which are η_{en} and $\Delta\eta_{\mathrm{ex}}$. Based on Luminosu *et al.* [12] method, following relations can be used for error analysis:

$$\Delta\eta_{\mathrm{ex}} \quad \frac{\Delta\dot{I}}{\dot{E}x_{\mathrm{heat}}} \quad \frac{\dot{I}\Delta\dot{E}x_{\mathrm{heat}}}{\dot{E}x_{\mathrm{heat}}^2} \tag{19}$$

and

$$\Delta\eta_{\mathrm{en}} \quad \frac{\Delta\dot{q}_{\mathrm{a}}}{G_{\mathrm{c}}} \quad \frac{\dot{q}_{\mathrm{a}}\Delta G_{\mathrm{c}}}{G_{\mathrm{c}}^2} \tag{20}$$

where each error component can be evaluated through following relations:

$$\Delta Ex_{\mathrm{heat}} \quad \frac{\Delta T}{T_{\mathrm{s}}} \quad \frac{T_0\Delta T}{T_{\mathrm{s}}^2} \quad A_{\mathrm{c}}(\tau\alpha)G_{\mathrm{c}} \quad 1 \quad \frac{T_0}{T_{\mathrm{s}}} \quad A_{\mathrm{c}}(\tau\alpha)\Delta G_{\mathrm{c}} \tag{21}$$

$$\Delta\dot{I} \quad T_0\Delta\dot{S}_{\mathrm{gen}} \quad \dot{S}_{\mathrm{gen}}\Delta T \tag{22}$$

$$\Delta\dot{S}_{\mathrm{gen}} \quad \mathrm{R}\ln\frac{P_{\mathrm{out}}}{P_{\mathrm{in}}} \quad C_{\mathrm{p}}\ln\frac{T_{\mathrm{in}}}{T_{\mathrm{out}}} \quad C_{\mathrm{p}}\frac{T_{\mathrm{out}} \quad T_{\mathrm{in}}}{T_0} \quad \Delta\dot{m} \quad G_{\mathrm{c}}A_{\mathrm{c}}(\tau\alpha)\frac{\Delta T}{T_0^2}$$

$$\dot{m}C_{\mathrm{p}} \quad \frac{1}{T_{\mathrm{out}}} \quad \frac{1}{T_{\mathrm{in}}} \quad \frac{2}{T_0} \quad \frac{(T_{\mathrm{out}} \quad T_{\mathrm{in}}}{T_0^2} \quad \Delta T \quad \dot{m}\mathrm{R} \quad \frac{1}{P_{\mathrm{out}}} \quad \frac{1}{P_{\mathrm{in}}} \quad \Delta P \quad A_{\mathrm{c}}(\tau\alpha) \quad \frac{1}{T_{\mathrm{s}}} \quad \frac{1}{T_0} \quad \Delta G_{\mathrm{c}} \tag{23}$$

$$\Delta\dot{q}_{\mathrm{a}} \quad C_{\mathrm{p}} \quad \frac{\Delta\dot{m}(T_{\mathrm{out}} \quad T_{\mathrm{in}}) \quad 2\dot{m}\Delta T}{A_{\mathrm{c}}} \tag{24}$$

Results and discussions

The errors in the measuring of temperature, mass flow rate, pressure, and solar radiation are 1 °C, $2.4\cdot10^{-5}$ kg/s, ±1%, and 1.25 W/m^2, respectively. Therefore the maximum errors of indirect measuring of energy and exergy efficiencies estimated to be 0.03 and ±0.13 using eqs. (19) and (20).

We have used the average of daily measurements during a winter 2005. The experiments are done for 8 hours a day from 8:00 a. m. to 4:00 p. m.. The number of clear sky days for winter 2005 was 76. Note that the radiation flux was not constant everyday during the winter days but our aim was to study the average results for the whole winter during the sunny days.

Figure 3 shows the average solar radiation intensity, captured by the vertically installed solar collector, and the ambient temperature in °C *vs*. daytime in winter. The experimental results for a random month (February) have been added to the plots for comparison. The maximum average solar radiation absorbed by the flat plate solar collector is occurring around noon from 12:00 to 13:30 local time. Its average decreases slowly and reaches to 400 W/m^2 at 4:00 p. m. during the winter. Figure 3 shows that solar radiation in the clear sky, captured by the flat plate solar collec-

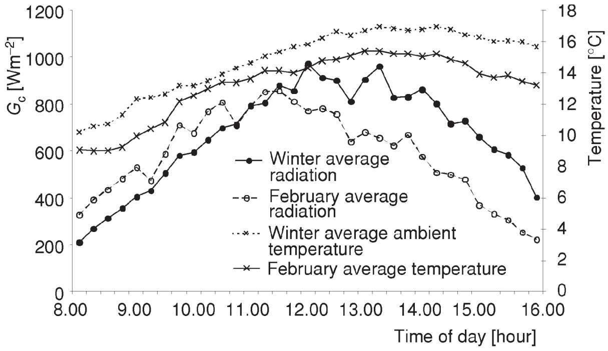

Figure 3. Average radiation intensity and ambient temperature in winter

Table 2. Average wind speed in winter and February [ms^{-1}]

Time of day	8:00	10:00	12:00	14:00	16:00
Winter	1.1	1.3	1.3	1.5	1.2
February	1.1	1.4	1.1	1.4	0.9

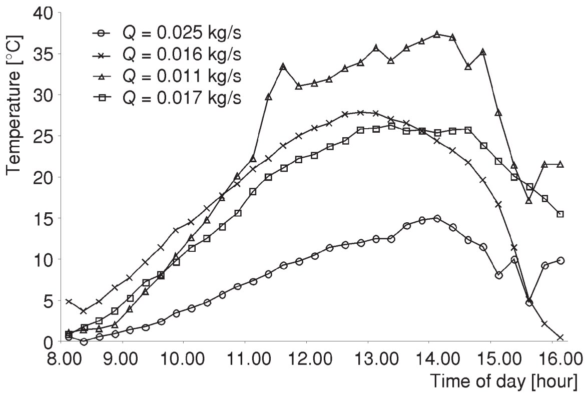

Figure 4. Average air temperature variation in winter at different flow rates

tor, is more than 600 W/m^2 during the time period of 10:00 a. m. until 3:00 p. m.. It is a good indication of the solar potential energy in the test region.

In winter, the average ambient temperature increases and reaches to its maximum of 17 °C from 14:00 to 14:30; it decreases with decreasing solar radiation. The average ambient temperature starts from 10 at 8:00 a. m. and reaches its highest value of 17 °C at 2:30 p. m. and falls down to 15.5 °C at 4:00 p. m. in the winter. The average temperature plot shows how cold is the winter in the place that solar air collector was tested to give a good basis for study on performance of such solar collectors.

The average wind speed during the winter and February at 8:00, 10:00, 12:00, 14:00, and 16:00 during day are recorded in tab. 2. The minimum and maximum values of average wind speed are 1.1 m/s at 8:00, and 1.5 m/s at 14:00, respectively for the winter. For February, the minimum and maximum values of average wind speed recorded are 0.9 m/s at 16:00, and 1.4 m/s at 10:00 and 14:00, respectively.

Figure 4 shows the average temperature variation of air as working fluid in the solar air collector during the winter as a function of day time at different mass flow rates. It can be seen that the lower mass flow rate causes the higher air temperature variation along the day. The physical meaning of this phenomenon is, having constant available heat source (solar radiation), in lower mass flow rates, the flowing air has more time to gain the heat energy from the absorber surface, which causes more increase in its temperature.

The minimum mass flow rate of air should be selected such that the air circulates enough in the room during the day; furthermore, higher flow rate may cause some discomfort for occupants. The optimum mass flow rate depends also on the ambient conditions such as ambient temperature and solar radiation energy.

The average variation of useful power produced by the solar air collector is plotted *vs.* day time during the winter and February for visual comparison in fig. 5. The mass flow rateo of

$\dot{m}_a = 0.015$ kg/s is selected for calculation of useful power. According to the fig. 5, from 11:00 to 15:00 the absorbed energy is the highest amount during the day and it is hold for both graphs, *i. e.* average useful energy in winter and February. It can be interpreted from fig. 5 that the minimum useful power during the winter occurs at 8:00 a. m. at the value of 15 W/m^2 and this value increases sharply to 190 W/m^2 at noon and then remains constant with some low fluctuations until 14:30. From 14:30, it decreases and reaches to 90 W/m^2 at 16:00. The same trend also happens for the average useful energy in the February month. It should be noticed that this value is the useful energy produced per unit area of collector.

Figure 6 shows the average energy efficiency of the solar air collector during the day at different mass flow rates. Such graphs can be used for optimizing the mass flow rate for the best energy efficiency for this collector. From the experimental data, it can be observed that the energy efficiency affected mainly by mass flow rate and temperature increase during the day that the latter parameter is a function of solar radiation, wind speed, and ambient temperature. It means that all of these parameters can affect the energy efficiency. From fig. 6 it can be concluded that the highest mass flow rate of $\dot{m}_a = 0.025$ kg/s has the lowest energy efficiency and mass flow rate of $\dot{m}_a = 0.016$ kg/s has the highest average energy efficiency during the day. It is noticeable that energy efficiency of $\dot{m}_a = 0.011$ kg/s is lower than $\dot{m}_a = 0.016$ kg/s and $\dot{m}_a = 0.017$ kg/s but higher than $\dot{m}_a = 0.025$ kg/s.

In fig. 7 the variation of irreversibility has been plotted *vs.* day time at different mass flow rates. It can be

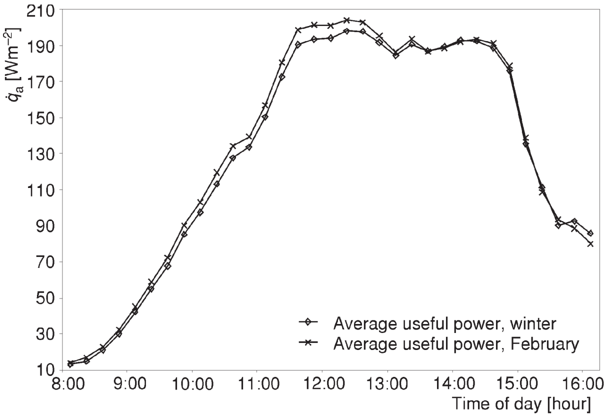

Figure 5. Average useful energy during winter, $\dot{m}_a$ = 0.015 kg/s

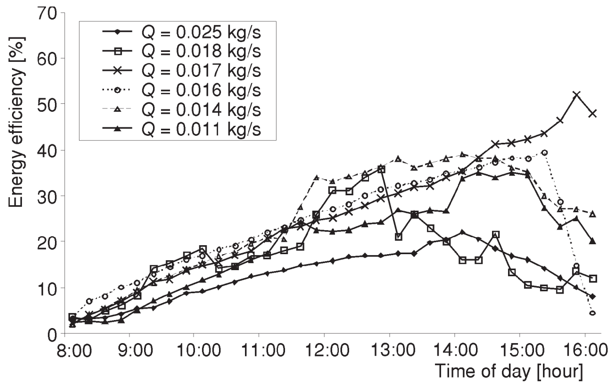

Figure 6. Energy efficiency during winter as a function of day time at different flow rate

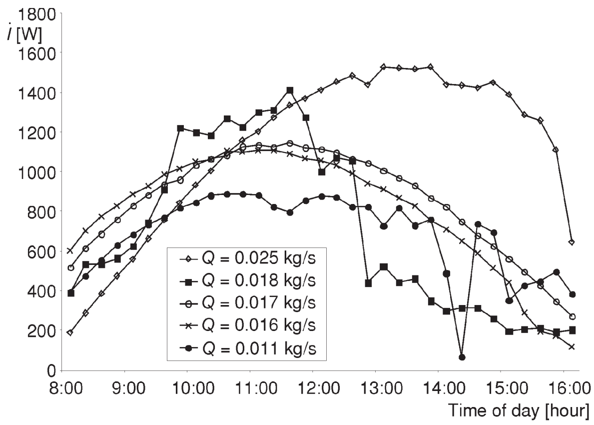

Figure 7. Irreversibility during winter for different mass flow rates *vs.* day time

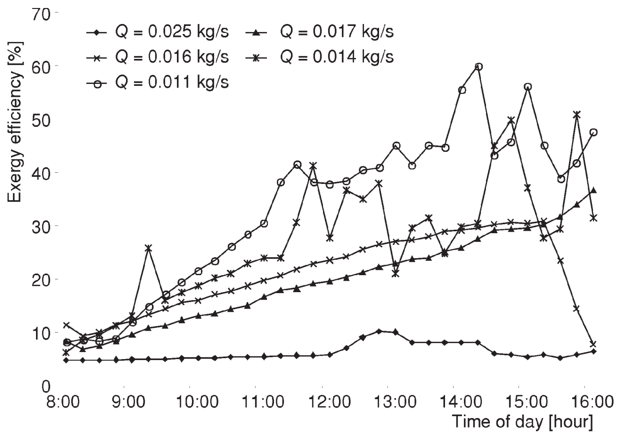

Figure 8. Exergy efficiency during winter per different mass flow rates in the day times

seen that mass flow rates of $\dot{m}_a$ = = 0.016 kg/s and $\dot{m}_a$ = 0.017 kg/s follow the same pattern while the latter flow rate has a slightly higher irreversibility most of the time. They also reach to their maximum value at noon to 1100 W for this collector. The highest mass flow rate of $\dot{m}_a$ = 0.025 kg/s has the highest irreversibility during the test time that reaches to its maximum value of 1500 W at 13:30, and then decreases to 610 W at 16:00.

From fig. 8 it can be seen easily that in the flow rate of 0.011 kg/s to 0.025 kg/s, the maximum flow rate has the lowest and the minimum flow rate has the highest exergy efficiency. Obviously this is not hold for every mass flow rate and there might be an optimum flow rate less than 0.011 kg/s bellow which decreasing of flow rate cause the exergy efficiency to decrease. The range of studied flow rate was selected so that it meets the required criteria of building HVAC system.

For the mass flow rate of $\dot{m}_a$ = 0.111 kg/s, the exergy efficiency started from 9% at 8:00 and it increases slowly to 51% at 14:00 and then followed by a sudden jump to reach its maximum of around 85% at 14:45 and then decreasing with some fluctuations to 40% at 16:00. The curves in fig. 8 indicates that the higher mass flow rate, the higher second law efficiency.

It can be seen that the minimum exergy efficiency belongs to the higher mass flow rate and the mass flow rate of $\dot{m}_a$ = 0.111 kg/s has the highest exergy efficiency in our experiments.

Summary and conclusion

A solar flat plate air collector was manufactured and connected to a room as the model to study the possibility of using such solar heating system in the northern parts of Iran. This collector was tested as a solar air heater to see how good it could be for warming up the test room during a winter. The experimental data obtained through accurate measurements during a winter were analyzed using energy and energy analysis to find the optimum mass flow rate, which leads to the maximum exergy efficiency. An exergy analysis showed that entropy is generated in solar air heating due to the friction of fluid flow, heat transfer between warm walls of collector and environment, heat transfer between sun surface and absorbing surface, and temperature change of passing air. It was found that for the test setup at the test location, among the different tested mass flow rates, a mass flow rate of 0.0011 kg/s is the optimum for tested conditions which leads to the highest second law efficiency. It was pointed out that the maximum irreversibility, occurs at noon, when solar radiation is maximum; it decreases as solar energy decreases.

Nomenclature

A	– absorbing area, [m^2]	h	– enthalpy, [kJkg^{-1}]
C	– specific heat, [kJkg^{-1}K^{-1}]	$\dot{I}$	– irreversibility, [kW]
$\dot{E}x$	– rate of exergy, [kJs^{-1}]	$\dot{m}$	– mass flow rate, [kgs^{-1}]
G	– solar radiation flux, [kWm^{-2}]	p	– pressure, [Pa]

$\dot{Q}$ – rate of heat energy received, [kW]
$\dot{q}$ – ratio of heat energy received by the unit area, [kWm^{-2}]
R – gas constant for carrier fluid, [kJkg^{-1}K^{-1}]
$\dot{S}$ – rate of entropy generated, [kWK^{-1}]
T – temperature, [K]

Greek letters

Δ – error in measuring or calculation
η – efficiency, [–]
$\tau\lambda$ – absorbance-transmittance product, [–]
en – energy
ex – exergy

Subscripts

a – carrier fluid (air)
c – collector
d – daily
gen – generated
heat – heat energy
i – hourly
in – inlet flow of carrier fluid
out – outlet flow of carrier fluid
p – constant pressure
s – sun
work – work
0 – ambient

References

[1] Perrot, P., A to Z of Thermodynamics, Oxford University Press, Oxford, UK, 1998
[2] Rant, Z., Exergy, a New Word for Technical Available Work (in German), *Forschung auf dem Gebiete des Ingenieurwesens, 22* (1956), pp. 36-37
[3] Gibbs, J. W., A Method of Geometrical Representation of Thermodynamic Properties of Substances by Means of Surfaces: Reprinted in Gibbs, Collected Works (Eds. W. R. Longley, R. G. Van Name), Transactions of the Connecticut Academy of Arts and Sciences, *2* (1931), pp. 382-404
[4] Moran, M. J., Shapiro, H. N., Fundamentals of Engineering Thermodynamics, 6th ed., John Wiley and Sons, New York, USA, 2007
[5] Van Wylen, G. J., Thermodynamics, John Wiley and Sons, New York, USA, 1991
[6] Wark, J. K., Advanced Thermodynamics for Engineers, McGraw-Hill, New York, USA, 1995
[7] Bejan, A., Advanced Engineering Thermodynamics, 2nd ed., John Wiley and Sons, New York, USA, 1997
[8] Saravan, M., Saravan, R., Renganarayanan, S., Energy and Exergy Analysis of Counter Flow Wet Cooling Towers, *Thermal Science, 12* (2008), 2, pp. 69-78
[9] Bejan, A., Kearney, D. W., Kreith, F., Second Law Analysis and Synthesis of Solar Collector Systems, *Journal of Solar Energy Engineering, 103* (1981), 1, pp. 23-28
[10] Bejan, A., Entropy Generation Minimization, CRC Press, Boca Raton, Fla., USA, 1996
[11] Londono-Hurtado, A., Rivera-Alvarez, A., Maximization of Exergy Output from Volumetric Absorption Solar Collectors, *Journal of Solar Energy Engineering , 125* (2003), 1, pp. 83-86
[12] Luminosu, I., Fara, L., Thermodynamic Analysis of an Air Solar Collector, *International Journal of Exergy, 2* (2005), 4, pp. 385-408
[13] Altfeld, K,. Leiner, W., Fiebig, M., Second Law Optimization of Flat-Plate Solar Air Heaters, Part I: The Concept of Net Exergy Flow and the Modeling of Solar Air Heaters, *Solar Energy, 41* (1988), 2, pp. 127-132
[14] Altfeld, K., Leiner, W., Fiebig, M., Second Law Optimization of Flat-Plate Solar Air Heaters, Part 2: Results of Optimization and Analysis of Sensibility to Variations of Operating Conditions, *Solar Energy, 41* (1988), 4 , pp. 309-317
[15] Torres-Reyes, E., *et al*., Optimal Process of Solar to Thermal Energy Conversion and Design of Irreversible Flat-Plate Solar Collectors, *Energy 28* (2003), 2, pp. 99-113
[16] Kurtbas, I., Durmus, A., Efficiency and Exergy Analysis of a New Solar Air Heater, *Renewable Energy, 29* (2004), 9, pp. 1489-1501
[17] Ajam, H., Farahat, S., Sarhaddi, F., Exergetic Optimization of Solar Air Heaters and Comparison with Energy Analysis, *International Journal of Thermodynamics, 8* (2005), 4, pp. 183-190
[18] Ucar, M. I., Thermal and Exergy Analysis of Solar Air Collectors with Passive Augmentation Techniques, *International Communications in Heat and Mass Transfer, 33* (2006), 10, pp. 1281-1290
[19] Esen, H., Experimental Energy and Exergy Analysis of a Double-Flow Solar Air Heater Having Different Obstacles on Absorber Plates, *Building and Environment, 43* (2008), 6, pp. 1046–1054
[20] Gupta, M. K., Kaushik, S. C., Exergetic Performance Evaluation and Parametric Studies of Solar Air Heater, *Energy, 33* (2008), 11, pp. 1691-1702

[21] Fujiwara, M., Exergy Analysis for the Performance of Solar Collectors, *Journal of Solar Energy Engineering, 105* (1983), 2, pp. 163-167
[22] Xiaowu, W., Ben, H., Exergy Analysis of Domestic-Scale Solar Water Heaters, *Renewable and Sustainable Energy Reviews, 9* (2005), 6, pp. 638-645
[23] Mohseni-Languri, E., Experimental and Dynamic Numerical Investigation on a Solar Air Heater, Thesis, Technical University of Noshiravani, Babol, Iran, 2007
[24] Duffie, J. A, Beckman, W. A, Solar Engineering of Thermal Processes, 2nd ed., John Wiley and Sons, New York, USA, 1991

Authors´ affiliations:

E. Mohseni-Languri, (**corresponding author**)
Department of Mechanical Engineering,
University of Wisconsin-Milwaukee, EMS,
3200 N. Cramer St., Milwaukee, WI 53211, USA
E-mail: Ehsan@uwm.edu

H. Taherian
Department of Mechanical Engineering,
Babol (Noshirvani) University of Technology, Iran

R. Masoodi , J. R. Reisel
Department of Mechanical Engineering,
University of Wisconsin-Milwaukee, EMS, USA

Paper submitted: September 6, 2008
Paper revised: November 19, 2008
Paper accepted: December 26, 2008